Inventory of Supplemental Information

The supplemental information includes 7 supplementary figures and 2 tables that provide controls and supporting data to the corresponding main figures, as well as a detailed version of the materials and methods used in this study.

Figure S1: Control reactions demonstrating ATP, PAN and 20S dependency of the degradation reaction presented in main Figure 1.

Figure S2: Quantitation of the spared RFP domain that accumulated upon *in vitro* proteasomal degradation of p21-RFP, RFP-p21, ova-RFP & RFP-ova (see main Figure 2).

Figures S3 & S4 Distinct and common peptides produced during proteasomal degradation of ovalbumin-RFP and RFP-ovalbumin and also of p21-RFP and RFP-p21 (raw data that was used to generate main Figure 5A).

Figure S5: Controls demonstrating that the MS analyses described in main Figure 5 were preformed when substrates were present in access and the rate of the proteasomal degradation was linear.

Figure S6: Calibration curve for the size exclusion column analysis presented in Figure 5B.

Figure S7: Alternative representation of the *in-silico* unraveling of MBP, ovalbumin and calmodulin.

Table S1: List of the MS detected heavy & light peptides used to generate Figure 5A.

Table S2: Mean Sizes of Peptides Generated by 26S from p21-RFP and RFP-p21.

Legends supplementary Figures:

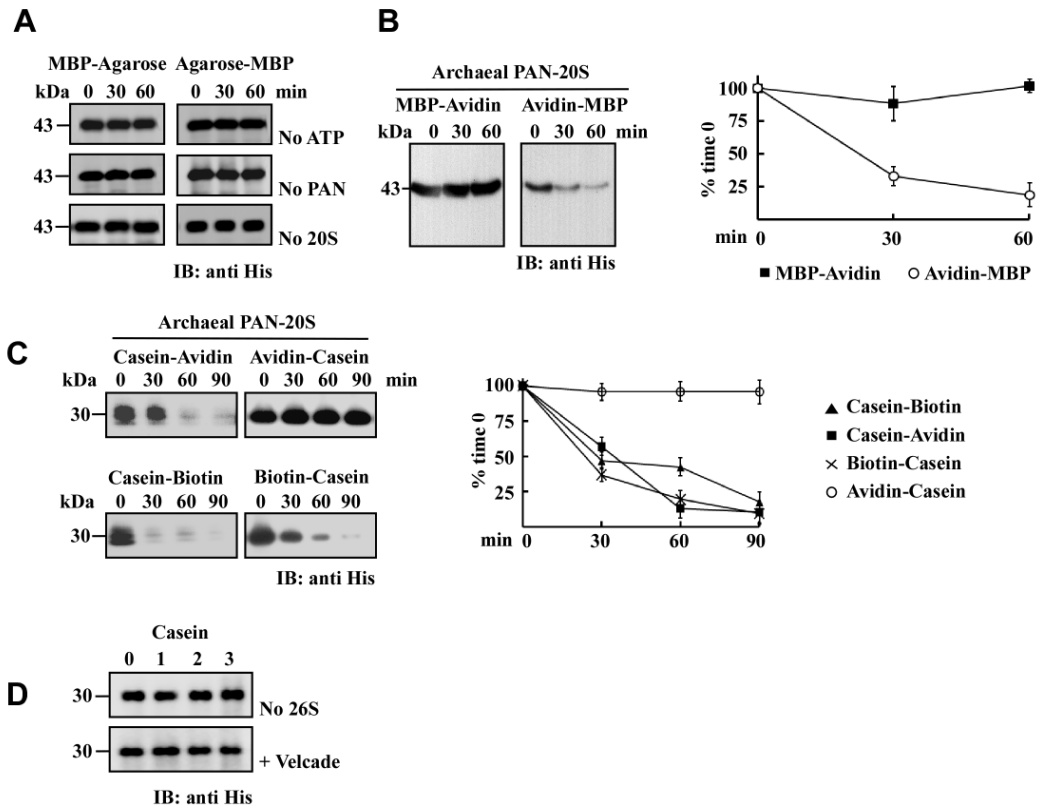

Figure S1: (A) Control reactions demonstrating ATP, PAN and 20S dependency of MBP-Agarose degradation. **(B)** Reaction mixture containing ATP, PAN, and proteasomes was added to MBP bound to streptavidin coated tubes through its C-(MBP-avidin) or N-terminus (avidin-MBP). The tubes were incubated at 55°C, at the designated time; a single tube was removed and washed three times. SDS sample buffer was added to the tubes, which were heated to 95°C for 5 minutes. Equal portions were separated by SDS-PAGE and analyzed as in A. **(C)** Time course of degradation of β-casein linked to biotin or avidin (attached to the biotin) on its N or C terminus as in A by the PAN-20S complex. **(D)** β-Casein is degraded in a proteasome dependent manner. β-Casein was incubated for the indicated time intervals in the absence of 26S proteasome and in the present of 26S proteasome and 2μM of the proteasome inhibitor, Velcade. Right: The remaining fraction of MBP or casein attached to agarose beads or streptavidin coated PCR tubes, through its C (square) or N-terminus (circle), at each time point is depicted on the right. SD were calculated from four repetitions under similar conditions.

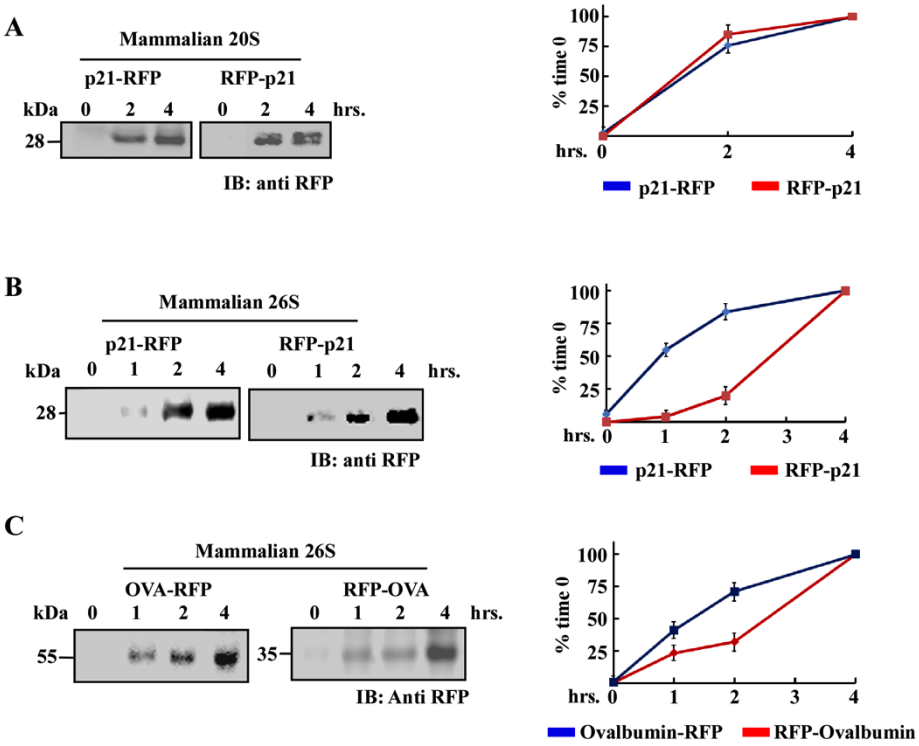

Figure S2: Generation over time of the RFP domain upon degradation of p21-RFP & RFP-p21 by the 20S proteasomes. (A) p21-RFP & RFP-p21 by the 26S proteasomes **(B),** and ovalbumin-RFP & RFP-ovalbumin by the 26S proteasomes **(C)**. These experiments are quantified on the right. SD were calculated from three repetitions under similar conditions.

A. Ovalbumin derived peptides generated from degradation of Ovalbumin-RFP and RFP-ovalbumin by the 20S proteasome

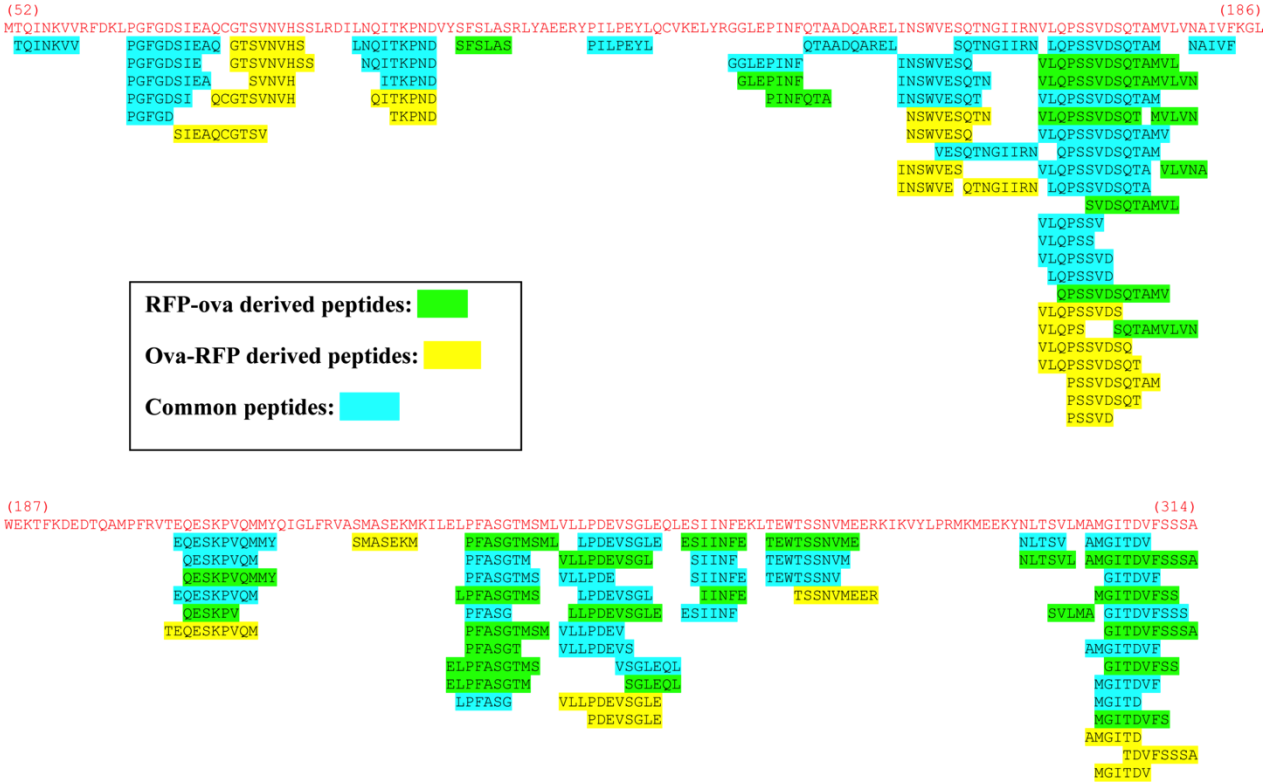

B. p21 derived peptides generated from degradation of p21-RFP and RFP-p21 by the 26S proteasome

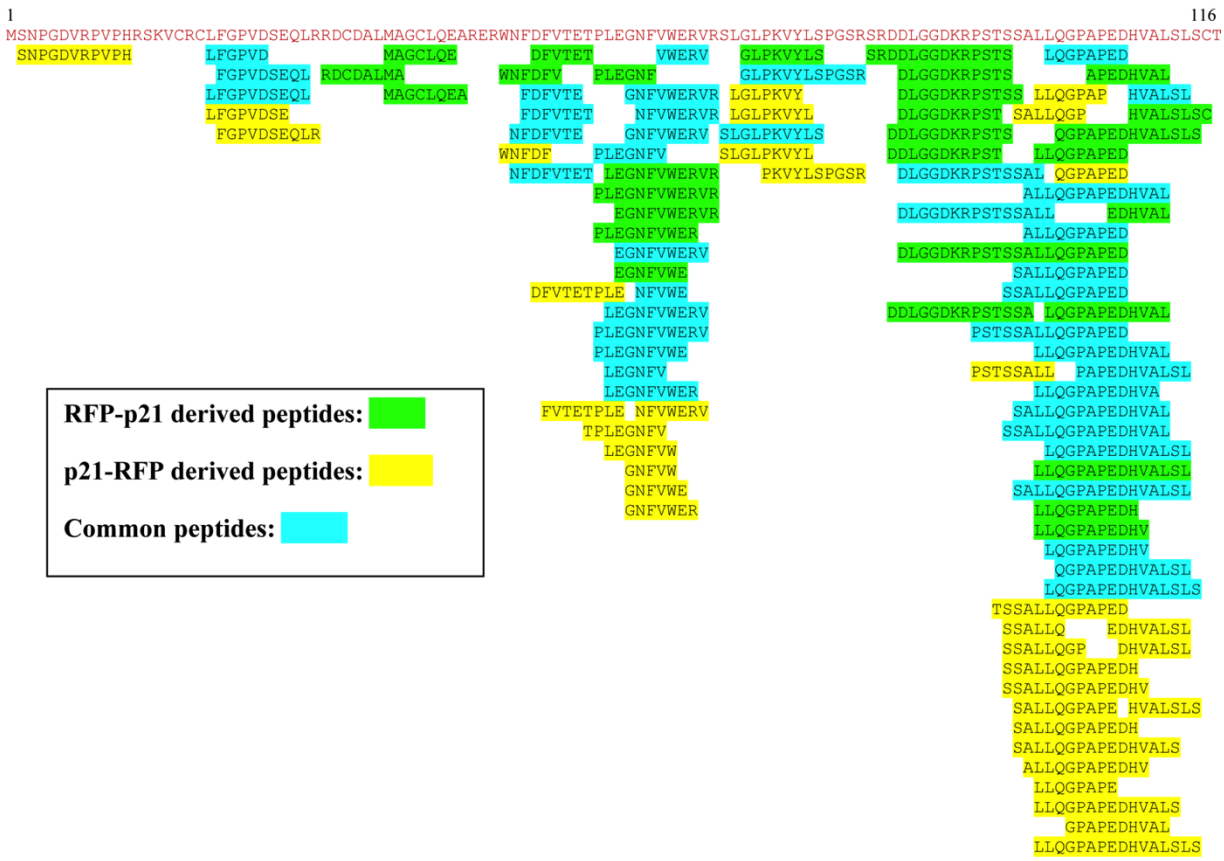

Figure S3: Distinct and common peptides produced during proteasomal degradation of ovalbumin-RFP and RFP-ovalbumin and also of p21-RFP and RFP-p21. Ovalbumin and p21 fused to RFP through either their C or N termini were incubated with purified rabbit 20S or 26S proteasomes at 37ºC for four hours. The products of the reactions were separated from undigested proteins and proteasomes by ultra-filtration through a 10 kDa membrane, and the products were determined by mass spectrometry analysis. **(A)** Ovalbumin-RFP compared with RFP-ovalbumin degraded by the 20S proteasome. The peptides are colored coded such that peptides derived only from RFP-ovalbumin are highlighted in green, peptides derived only from

ovalbumin-RFP are highlighted in yellow and peptides generated from both substrates are highlighted in blue. **(B)** Peptides generated from p21-RFP and RFP-p21 during degradation by the 26S proteasome. **(C)** Products of degradation of p21-RFP and RFP-p21 by the 20S proteasome. Unique RFP-p21 derived peptides are highlighted in green, unique p21-RFP derived peptides are highlighted in yellow and common peptides are highlighted in blue.

Peptide sequence	**P21-RFP=H RFP-p21=L**	**P21-RFP=L RFP-p21=H**
G.SRSRDDLGGDKRPSTS.S	0.48±0.02	0.46±0.02
P.G]SRSRDDLGGDK#RPST.S	0.81±0.15	0.96±0.15
L.S]PGSRSRDDLGGDK#RPST.S	0.875±0.645	1.52±0.645
A.S]NPGDVRPVPHRS.K	9.14±0.86	10±0.86
A.SNPGDVRPVPHRS.K	9.14±0.86	10±0.86
L.GGDKRPSTSSAL.L	0.83±0.1	0.93±0.1
T.L]VSERPED.S	0.59±0.06	0.65±0.06
Y.L]SPGSRSRDDLGGDK#RPSTSSA.L	1.25±0.105	1.145±0.105
C.TLVSERPED.S	0.72±0.14	0.58±0.14
C.T]LVSERPED.S	0.72±0.14	0.58±0.14
L.L]QGPAPED.H	0.43±0.035	0.395±0.035
L.LQGPAPED.H	0.43±0.035	0.395±0.035
A.LLQGPAPEDH.V	0.435±0.045	0.48±0.045
C.T]LVSERPEDSPGGPGTSQGR.K	0.175±0.035	0.14±0.035
L.TDFYHS.K	0.13±0.06	0.19±0.06
L.T]DFYHS.K	0.13±0.06	0.19±0.06
L.L]QGPAPEDHV.A	0.365±0.005	0.36±0.005
L.QGPAPEDHVALS.L	0.61±0.27	0.34±0.27
A.LLQGPAPED.H	0.52±0.26	0.78±0.26
A.L]LQGPAPED.H	0.52±0.26	0.78±0.26
Q.G]PAPEDHVAL.S	0.27±0.03	0.24±0.03
Q.GPAPEDHVAL.S	0.27±0.03	0.24±0.03
D.HVALSLS.C	13.43±3.24	16.67±3.24
A.L]LQGPAPEDHV.A	0.71±0.33	1.04±0.33
L.Q]GPAPEDHVAL.S	0.74±0.19	0.93±0.19
L.QGPAPEDHVAL.S	0.72±0.07	0.65±0.07
F.D]FVTET.P	0.365±0.065	0.3±0.065
L.LQGPAPEDHVALS.L	0.185±0.005	0.19±0.005
R.RQTSLTDFYHS.K	1.735±2.435	4.17±2.435
S.ALLQGPAPED.H	4.95±1.3	6.25±1.3
L.GLPKVYLSPGSR.S	0.56±0.13	0.69±0.13
L.G]LPK#VYLSPGSR.S	0.57±0.12	0.69±0.12
T.SSALLQGPAPED.H	1.315±1.065	2.38±1.065
T.S]SALLQGPAPED.H	1.315±0.175	1.14±0.175
S.SALLQGPAPED.H	2.985±1.565	4.55±1.565
S.S]ALLQGPAPED.H	3.03±1.52	4.55±1.52
D.D]LGGDK#RPSTSSALLQGPAPED.H	0.445±0.195	0.64±0.195
D.DLGGDKRPSTSSALLQGPAPED.H	0.435±0.2	0.64±0.2
E.GNFVWERVR.S	6.4±6.1	12.5±6.1
A.LLQGPAPEDHVALS.L	0.4±0.03	0.43±0.03
L.LQGPAPEDHVAL.S	0.545±0.29	0.84±0.29
P.LEGNFV.W	2.195±0.585	2.78±0.585
L.QGPAPEDHVALSLS.C	1.73±0.12	1.85±0.12
C.LFGPVD.S	1.275±0.085	1.19±0.085
D.FVTETPLE.G	3.765±3.385	7.15±3.385
L.GLPKVYLS.P	0.44±0.2	0.64±0.2
A.L]LQGPAPEDHVAL.S	0.82±0.25	1.07±0.25
Q.GPAPEDHVALSL.S	0.375±0.1	0.48±0.1
Q.G]PAPEDHVALSL.S	0.375±0.1	0.48±0.1

L.Q]GPAPEDHVALSL.S	1.23±0.29	1.52±0.29
L.QGPAPEDHVALSL.S	1.23±0.29	1.52±0.29
L.LQGPAPEDHVALSLS.C	0.405±0.275	0.68±0.275
L.L]QGPAPEDHVALSLS.C	0.405±0.275	0.68±0.275
R.SLGLPKVY.L	0.69±0.22	0.91±0.22
L.GLPKVYL.S	0.595±0.085	0.68±0.085
L.F]GPVDSEQL.R	0.5±0.01	0.51±0.01
L.FGPVDSEQL.R	0.5±0.14	0.64±0.14
S.ALLQGPAPEDHVAL.S	2.17±0.17	2±0.17
T.SSALLQGPAPEDHVAL.S	1.82±0.68	2.5±0.68
T.S]SALLQGPAPEDHVAL.S	1.82±0.46	2.28±0.46
A.LLQGPAPEDHVALSLS.C	1.685±0.515	1.17±0.515
S.SALLQGPAPEDHVAL.S	3±1.55	4.55±1.55
S.S]ALLQGPAPEDHVAL.S	3±1.17	4.17±1.17
L.LQGPAPEDHVALSL.S	1.01±0.34	1.35±0.34
L.L]QGPAPEDHVALSL.S	1.01±0.34	1.35±0.34
F.D]FVTETPLE.G	0.325±0.065	0.26±0.065
N.F]DFVTE.T	0.385±0.025	0.36±0.025
F.DFVTETPLE.G	0.325±0.065	0.26±0.065
L.EGNFVWERV.R	2.37±0.97	3.34±0.97
N.F]DFVTET.P	0.395±0.115	0.51±0.115
N.FDFVTET.P	0.395±0.115	0.51±0.115
A.LLQGPAPEDHVALSL.S	0.86±0.18	1.04±0.18
A.L]LQGPAPEDHVALSL.S	0.855±0.015	0.84±0.015
W.N]FDFVTE.T	1.36±0.37	1.73±0.37
C.LFGPVDSEQL.R	0.85±0.12	0.73±0.12
W.NFDFVTE.T	1.36±0.31	1.67±0.31
W.N]FDFVTET.P	2.78±0.79	3.57±0.79
P.LEGNFVWERV.R	5.56	5.56
T.SSALLQGPAPEDHVALSL.S	2.29±0.49	2.78±0.49
S.SALLQGPAPEDHVALSL.S	2.88±2.68	5.56±2.68
S.S]ALLQGPAPEDHVALSL.S	2.88±2.68	5.56±2.68
V.TETPLEGNFVWERV.R	0.87±0.45	1.32±0.45
V.T]ETPLEGNFVWERV.R	0.87±0.41	1.28±0.41
E.TPLEGNFVW.E	8.965±2.7	6.25±2.7
V.TETPLEGNFVW.E	0.705±1.145	1.85±1.145
R.WNFDFVTE.T	15.26±5.26	10±5.26
N.FDFVTE.T	0.375±0.015	0.36±0.015
T.S]SALLQGPAPEDHVALSL.S	2.29±0.49	2.78±0.49

Figure S4: Ratios and SD of individual peptides obtained upon comparative MS analyses of peptides produced during degradation by 26S proteasomes of p21 blocked on its C-terminus (p21-RFP) or its N-terminus (RFP-p21). Isotopic ratios of individual peptides upon labeling of p21-RFP or RFP-p21degradation products with heavy formaldehyde are presented. These experiments were repeated three times with SD of less than 10%.

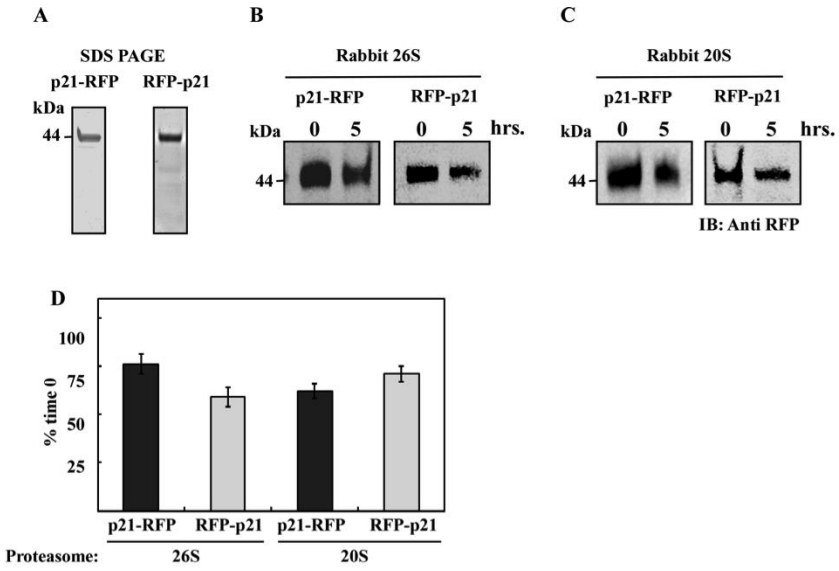

Figure S5: Substrate was present in excess during proteasomal degradation reactions where products analyzed by mass spectrometry. Therefore, products were probably generated directly from the protein rather than in repeated cycles through the proteasome. **(A)** Coomassie stain SDS -PAGE of purified p21-RFP and RFP-p21 used in the degradation assays. **(B)** Western blot analysis of equal volumes removed from p21-RFP and RFP-p21 26S degradation assay. **(C)** Western blot analysis of equal volumes removed from p21-RFP and RFP-p21 20S degradation assay. **(D)** Quantification of the final amounts of p21-RFP and RFP-p21in the proteasomal degradation assays presented in **(A)** & **(B)**. SD were calculated from three repetitions under similar conditions.

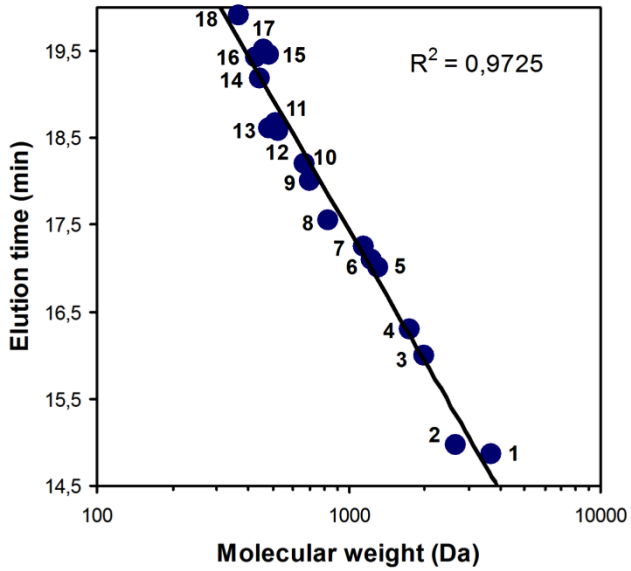

1	INSULIN B	10	AGFM
2	INSULIN A	11	LGG
3	SGLEQLESIINFEKL	12	FA
4	EQLESIINFEKL	13	AL
5	ASNENMETM	14	F
6	SIINFEKL	15	W
7	IINFEKL	16	M
8	YGGFL	17	Y
9	GGFL	18	A

Figure S6: Calibration curve for polyhydroxyethyl aspartamide size exclusion column, using fluorescamine-derivatized amino acid and peptide molecular weight standards. The typical peak width of these amino acids and peptides was 0.7 min.

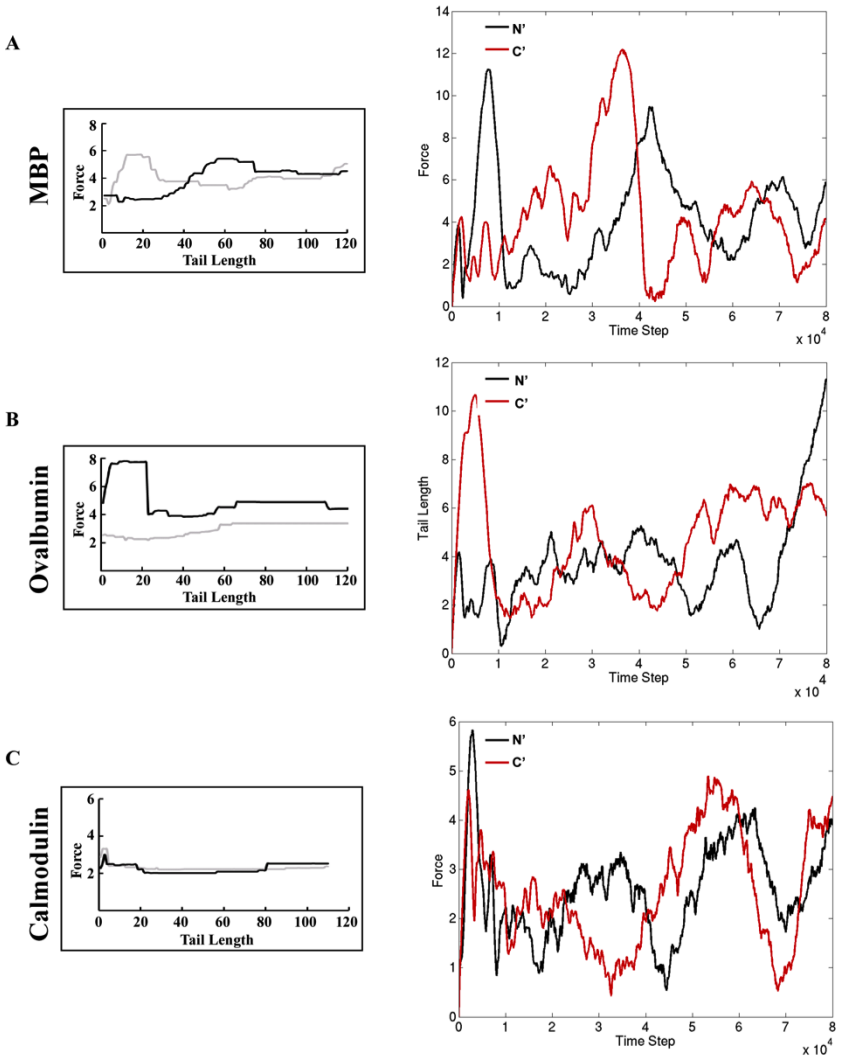

Figure S7: Alternative representation of the *in-silico* unraveling of MBP, ovalbumin and calmodulin. The graphs represent the average cumulative force that is applied to move a virtual spring, while pulling each protein from its N (gray) or C (black) terminus, demonstrating the unraveling of the termini at the indicated step. The calculations were performed for MBP **(A)**, Ovalbumin **(B)** and Calmodulin **(C)**. On the right is the force that was monitored on the moving virtual spring that was attached to the N' (black) or C' (red) terminus.

Table S1: Distinct and common products detected upon proteasomal degradation of ovalbumin-RFP versus RFP-ovalbumin and p21-RFP versus RFP-p21*.

Substrate	Proteasomes	peptides	Unique peptides	Common peptides
OVA-RFP	**20S**	***116***	***38 (33% ±8%)***	***78 (67% ±10%)***
RFP-OVA	**20S**	***119***	***41 (34% ±10%)***	***78 (66% ±7%)***
P21-RFP	**26S**	**91**	***44 (48% ±7%)***	***47 (52% ±9%)***
	20S	**56**	***33 (59% ±10%)***	***23 (41% ±10%)***
RFP-P21	**26S**	**84**	***37 (44% ±10%)***	***47 (56% ±8%)***
	20S	**46**	***23 (50% ±7%)***	***23 (50% ±8%)***

***The data is based on the MS analysis presented in Figure S6.

Table S2: Mean Sizes of Peptides Generated by 26S from p21-RFP and RFP-p21.

Substrate	Mean	S.E.M.	Range (of the means)	Median	S.E.Me.
P21-RFP	5.88	0.08	5.78-6.03	3.86	0.06
RFP-P21	5.89	0.52	6.93-5.36	3.96	0.13

Table S2: Mean sizes and median were calculated from the distributions of products obtained by size exclusion chromatography, assuming an average molecular weight of 110Da for each residue and the values are averages of three measurements. S.E.M., standard error of the mean; S.E.Me., standard error of the medians.

Supplemental experimental procedures

Generation and purification of proteasomal substrates

Bovine β-casein and the *E. coli* Maltose Binding Protein (MBP) were amplified by PCR and cloned in between MscI and XhoI sites downstream of the pelB leader sequence (β-casein) and NdeI and Xho I (MBP) sites of pET22B (Novagene) (termed pET22-casein and pET22-MBP). The primer corresponding to the N-terminus was designed to add 7 histidine residues upstream of the second amino acid of the gene, and the primer corresponding to the C-terminus of the gene was designed to add in frame a cysteine residue followed by a stop codon. For the N-terminal cysteine, the N-terminal primer was designed to insert a cysteine codon as the second encoded amino acid and the primer corresponding to the C-terminus was designed to add 7 histidine residues followed by a stop codon.

Calmodulin (xenopus), mouse p21 and the ovalbumin without a signal peptide were amplified by PCR and cloned in frame upstream or downstream of the entire sequence of RFP between the NdeI and XhoI sites of pET22 (Novagene). The primer corresponding to the N-terminus was designed to add 7 histidine residues upstream of the second amino acid of RFP sequence, while calmodulin, ovalbumin or p21 were fused to the C-terminus of RFP. Alternatively, the primer corresponding to the C-terminus was designed to add 7 histidine residues followed by a stop codon, while those proteins were fused to the N-terminus of RFP. The sequences of final plasmids were confirmed by sequencing.

Substrates

Plasmids were transformed into *E. coli* (BL-21 DE3). The bacteria were initially grown overnight in 50 ml LB medium containing 100 μg ampicillin/ml and used to inoculate two liters of culture that were grown until an optical density of 0.6 at 600 nm. Protein expression was

induced by IPTG addition (0.5 mM final concentration) and grown for an additional 3 hours. The bacteria (all but β-casein) were harvested by centrifugation, resuspended in 20 mM Hepes, pH7.5, 20 mM immidazole and lysed by sonication. The lysate was cleared by centrifugation at 14,000 rpm for 30 minutes at 4^{o}C, and the supernatant was loaded on Ni-NTA column. Following adsorption, the column was washed with 20 mM Hepes, pH 7.5, 1M NaCl, 1% Tween 20, and the bound proteins were eluted with 0.5 M imidazole in PBS. The eluted proteins were concentrated by ultrafiltration and fractionated on Superdex 75 column, while MBP was affinity purified on amylose resin (NEB). The relevant fractions were pooled, concentrated by ultrafiltration (Millipore), and stored at -70ºC until further use.

The pellet of bacteria expressing β-casein was resuspended in 20 mM Hepes, pH 7.5, 20 mM, 0.5% Tween 20 and lysed by sonication. The lysate was then centrifuged at 20,000g for 30 min, and the casein-containing pellets were resuspended in 50mM Hepes pH7.5, 6M guanidine-HCl. The lysate was cleared by centrifugation and the supernatant loaded on Ni-NTA column. Following adsorption, the column was washed with 50mM Hepes pH7.5, 6M guanidine-HCl and then with 20 mM Hepes, pH 7.5, 1M NaCl, 1% Tween 20 and the bound proteins were eluted with 0.5 M imidazole in PBS. The eluted protein were concentrated by ultrafiltration and fractionated on Superdex 75 column. The relevant fractions were pooled, concentrated by ultrafiltration (Millipore), and stored at -70ºC.

Degradation assays with pure proteasomes

Degradation of substrates by the mammalian 20S proteasome was performed at 37ºC in a buffer containing 50 mM Hepes pH 7.5, 5mM $MgCl_2$ and 1 mM DTT in the presence (for β-Casein and ovalbumin) or in the absence (for p21) of 0.018% SDS. Degradation of substrates by the mammalian 26S proteasome was performed at 37ºC with 50mM Hepes, pH 7.5, 5mM $MgCl_2$, 1mM DTT and 2mM ATP. For degradation of substrates by the archaeal 20S-PAN complex,

substrates were incubated at 55ºC with buffer containing 50mM Hepes, pH 7.5, 5mM $MgCl_2$, 30mM KCl, 1mM DTT and 2mM ATP. The molar ratio of proteasomes to substrates was 1:1000 (1nM proteasome per 1μM substrate) for all degradation reactions. Samples from the reaction mixture were removed at different time intervals and subjected to immunoblot analysis with the indicated antibodies. The immunoblots were quantified by densitometry (Quantity One, Bio-Rad).

Western Blot

Protein samples were boiled for 5 min in 2× Laemmli sample buffer, separated on a 10% nonreducing SDS polyacrylamide gel, and transferred onto a nitrocellulose membrane. The membrane was blocked for 30 minutes at room temperature in 5% BSA in TBST (50 mM Tris-HCl [pH 7.5], 100 mM NaCl, and 0.005% Tween-20), washed twice with PBS, and incubated for 2 h with the primary Ab. The membrane was then washed 4 times for 4 min each with TBST and incubated for 1 h with the secondary peroxidase-conjugated Ab, washed 4 times for 4 min each with TPBS, and then developed using chemiluminescence reagent kit (Amersham Pharmacia Biotec). Chemiluminescence signal was acquired by BioRad ChemiDoc XRS using long lasting ECL solution (BioRad), while verifying that none of the quantified bands were in saturation.

Chemidoc-Quantity-One software (Biorad Laboratories) was used to perform quantitative analyses.

Antibodies

For His immunoblot analysis, rabbit polyclonal IgG anti His-probe (H-15), (Santa Cruz Biotechnology) was used at 1:10, 000 dilution. For RFP immunoblot analysis, homemade rat

polyclonal antibodies were used at 1:4000 dilution. For Actin immunoblot analysis, mouse monoclonal IgG1 antibodies (ICN Biomedicals) were used at 1:10,000 dilution.

Quantitative comparison of proteasomal degradation products of RFP-p21 and p21-RFP.

To compare the relative amounts of the similar peptides generated by the 20S and 26S proteasomes upon the degradation of RFP-p21 and p21-RFP we labeled the degradation products of one of these p21 derivatives with heavy formaldehyde while the products prepared from the other p21 derivative were labeled with light formaldehyde. Labeling of the peptides by reductive dimethylation was done in the presence of 100mM $NaCBH_3$ (Sterogene), by adding Light Formaldehyde (35% Frutarom) to one of the samples, and heavy formaldehyde (20% w/w, Cambridge Isotope laboratories cat#CDLM-4599-1,6.5M) to the other sample to a final concentration of 200mM at pH 8. After 1 hour incubation at room temperature, the pH were lowered to 6.4 and the reaction was incubated an additional hour. Neutralization was done with 25mM ABC for 30min, and equal amounts of the light and heavy peptides were mixed, desalted on C18 disposable column (Harvard Apparatus) and re-suspended in 0.1% formic acid.

The peptides were resolved by reverse-phase chromatography on 0.075 X 200-mm fused silica capillaries (J&W) packed with Reprosil reversed phase material (Dr Maisch GmbH, Germany). The peptides were eluted with linear (90 minutes) gradients of 5 to 45%, and 15 minutes at 95% acetonitrile with 0.1% formic acid in water at flow rates of 0.25 μl/min. Mass spectrometry was performed by the LTQ-Orbitrap mass spectrometer in a positive mode using repetitively full MS scan followed by collision induced dissociation (CID) of the 7 most dominant ion selected from the first MS scan.

The mass spectrometry data was analyzed using the Sequest 3.31 software (Thermo-Fisher) searching against the specific sequence of the protein. The quantitation was done using the PepQuant algorithm of Bioworks (Thermo-Fisher) and ”in house" software.

Quantitative size distribution determination of the degradation products

Peptides generated during proteasomal degradation of p21-RFP and RFP-p21 were separated from undigested protein by ultrafiltration through a 10kDa cutoff membrane (Pal USA) and lyophilized. The material was resuspended in 0.1 M Hepes buffer pH 6.8 and separated by size-exclusion chromatography, using a polyhydroxy-ethyl aspartamide column (0.46 X 20 cm, Poly LC, Columbia, MD), and an HP1100 HPLC (Hewlett-Packard) equipped with a fluorometer detector. The mobile phase was 0.2M sodium sulfate, 25% acetonitrile (pH 3.0; adjusted with phosphoric acid), with a flow rate of 0.125ml/min. For each analysis, 20µl of peptides solution were added to 10µl of fluorescamine (dissolved at 0.3 mg/ml in acetone). The reaction was terminated after 30s with 30µl of H_2O, and the sample was injected immediately into the HPLC column. To determine the apparent molecular mass of the peptides eluted, the column was calibrated before use with 18 standard amino acids and peptides in the 200±3500 Da range that had been derivatized with fluorescamine in the same manner as proteasomal degradation products. Prior control studies showed that retention times of these fluorescamine-derivatized products are highly reproducible, and linearly dependent on the logarithm of their molecular weights (Figure S6) and that recovery of amino acids and peptides of different lengths is quantitative.

***In silico* calculation of termini availability of the different substrate**

A coarse-grained model based on the native structure (Go-like potential) was used (Clementi et al., 2000) to simulate the mechanical unfolding of MBP, ovalbumin, and calmodulin proteins (PDB codes 1N3X, 1OVA, and 1CFC, respectively). We used a reduced representation of the protein in which each residue is represented by a single bead, and the energy function was based on the native topology of the protein. The Langevin equation of motion was applied on the protein to include the Brownian perturbations of the water. To pull the protein from one of its

termini, we connected both termini to a spring following the work of Cieplak and co workers (Cieplak et al., 2002; Cieplak and Marszalek, 2005). The end of one spring was fixed to its initial location, and the end of the other spring was moved with a constant velocity $v_p=5\cdot10^{-3}$Å/τ, where τ is the time step in the simulation. The springs were connected to the protein when it was in its native structure, and the moving spring was moved in the direction of the end-to-end vector of the native structure. The attached springs were harmonic with a spring constant $K_p=1$. During a simulation the spring was moved with a constant velocity and we monitored the instantaneous pulling force F which is the extension of the pulling spring times its force constant K_p. We repeated the simulations using lower constant velocity ($v_p=5\cdot10^{-4}$ Å/τ) at which pulling from the N- or C-terminus results with similar unfolding pathways. These simulations allow reversible unfolding; yet indicate which terminus unfolds more easily. The forces that were monitored on the spring while pulling either ends of the protein were similar (data not shown) and the unfolding pathway of the protein was the same regardless of the pulling direction. We point out that the conclusions from the simulations with low and high force constants are identical. All simulations were performed at low temperature.

To examine what is the preferred direction for mechanical unfolding of the protein, we pulled the protein from its N- and C-terminus. During these simulations, we monitored the braking and formation of the native contacts in the protein and thereby the length of the tail that was released from the protein. To find the length of the tail, we looked for the number of consecutive residues (starting from the pulled terminal of the protein) that at least one of their native contacts was broken. In addition to plotting the time evolution of the instantaneous force and the length of the extended tail, we plot the average force needed to achieve a tail of a certain length. Such an analysis mostly is useful to compare the averaged total force needed to get an unfolded tail when the pulling is performed either from the N-or the C-terminus.

References

Cieplak, M., Hoang, T.X., and Robbins, M.O. (2002). Thermal folding and mechanical unfolding pathways of protein secondary structures. Proteins *49*, 104-113.
Cieplak, M., and Marszalek, P.E. (2005). Mechanical unfolding of ubiquitin molecules. J Chem Phys *123*, 194903.
Clementi, C., Nymeyer, H., and Onuchic, J.N. (2000). Topological and energetic factors: what determines the structural details of the transition state ensemble and "en-route" intermediates for protein folding? An investigation for small globular proteins. J Mol Biol *298*, 937-953.